Iranian Journal of Numerical Analysis and Optimization
Vol. 16, No. 1, 2026, pp 170–187
https://doi.org/10.22067/ijnao.2025.94352.1679
https://ijnao.um.ac.ir/

Research Article

Qualitative and Numerical Analysis of a Time-Fractional Ebola Model in Population Dynamics

G. Saini, B. Ghosh*, and S. Chand

Abstract

Mathematical modeling of infectious diseases plays a vital role in understanding population dynamics and guiding control strategies. In this study, we formulate and analyze time-fractional Ebola virus model incorporating the Caputo derivative of order $\sigma \in (0, 1)$ to capture memory and nonlocal effects in disease transmission. This formulation is important as it extends classical integer-order models to more realistically describe the persistence and delayed response of infection dynamics. A comprehensive qualitative analysis is presented, establishing the existence, uniqueness, and Hyers–Ulam stability of the solution of the considered model. To obtain the numerical approximation, a robust finite difference scheme based on the classical

*Corresponding author

Received 10 July 2025; revised 18 October 2025; accepted 15 November 2025

Gaurav Saini
Center for Data Science, Department of Computer Science and Engineering, Siksha 'O' Anusandhan (Deemed to be University), India. e-mail: gauravsaini@soa.ac.in

Bappa Ghosh
Center for Artificial Intelligence and Machine Learning, Department of Computer Science and Engineering, Siksha 'O' Anusandhan (Deemed to be University), India. e-mail: bg12.ghosh@gmail.com

Sunita Chand
Department of Mathematics, Siksha 'O' Anusandhan (Deemed to be University), India. e-mail: sunitachand@soa.ac.in

How to cite this article
Saini, G., Ghosh, B. and Chand, S., Qualitative and Numerical Analysis of a Time-Fractional Ebola Model in Population Dynamics . *Iran. J. Numer. Anal. Optim.*, 2026; 16(1): 170-187. https://doi.org/10.22067/ijnao.2025.94352.1679

L1 discretization is developed. The resulting nonlinear system is efficiently solved using the Newton–Raphson iterative technique. The numerical results demonstrate that fractional-order models provide enhanced flexibility and accuracy compared to traditional integer-order formulations. Specifically, variation in the fractional order significantly influences the rate of infection and recovery, highlighting the crucial role of memory effects in epidemic modeling. These findings confirm that incorporating fractional derivatives offers improved insight into Ebola virus dynamics and can support more effective intervention and treatment strategies.

AMS subject classifications (2020): Primary 26A33, 37M05 ; Secondary 92D25, 65L05.

Keywords: Ebola virus, fractional order model, Caputo derivative, L1 technique, Qualitative analysis.

1 Introduction

Fractional calculus generalizes classical calculus by extending the concept of derivatives and integrals to noninteger (arbitrary) orders. This framework is particularly well-suited for describing systems with memory, hereditary effects, and long-range temporal dependencies. As a result, fractional differential equations (FDEs) have emerged as powerful tools in modeling a wide range of complex phenomena across various disciplines, including viscoelastic materials [23], anomalous diffusion processes [17], quantitative finance, and population dynamics [10, 9]. For comprehensive discussions on the theoretical foundations and applications of fractional calculus, one may refer to [18, 5] and references therein. Although FDEs often involve increased computational complexity due to their nonlocal nature, they offer a more accurate representation of systems where classical integer-order models fall short. The growing interest in fractional modeling reflects its ability to bridge the gap between empirical observations and theoretical predictions, making it a vital component of modern applied mathematics and scientific computing.

Population dynamics models provide mathematical frameworks to analyze how population sizes evolve under the influence of biological interactions, environmental conditions, and disease transmission [11]. These models are instrumental in fields such as ecology, epidemiology, and resource management, where they aid in understanding the spread of infectious diseases and formulating effective control and intervention strategies [12, 22]. Ebola virus, a highly virulent pathogen belonging to the Filoviridae family, causes Ebola virus disease (EVD), a severe and often fatal illness in humans and nonhuman primates. First identified in 1976 during simultaneous outbreaks in Sudan and the Democratic Republic of Congo near the Ebola River, the virus has since led to several deadly epidemics across sub-Saharan Africa. Ebola is primarily transmitted

through direct contact with the blood, secretions, organs, or other bodily fluids of infected individuals or contaminated materials. The incubation period ranges from 2 to 21 days, and symptoms include sudden onset of fever, fatigue, muscle pain, vomiting, diarrhea, and, often, internal and external bleeding. Currently, treatment for EVD is primarily supportive and includes rehydration, oxygen supplementation, and the management of clinical complications. In recent years, experimental therapies and vaccines have been introduced, among which the rVSV-ZEBOV vaccine has demonstrated notable efficacy in clinical trials. Mathematical models of Ebola virus transmission, often based on compartmental structures like the SEIR framework, are crucial tools for understanding outbreak dynamics and informing strategies for intervention, quarantine, vaccination, and public health preparedness.

The classical Ebola virus model for $t > 0$ is given as follows:

$$\begin{cases} \partial_t S(t) = -\alpha S(t)I(t) + \beta R(t) - \gamma N, \\ \partial_t I(t) = \alpha S(t)I(t) - \epsilon I(t) - \delta I(t), \\ \partial_t R(t) = \delta I(t) - \beta R(t), \\ \partial_t D(t) = \epsilon I(t) + \gamma N, \end{cases} \tag{1}$$

subject to the initial conditions

$$S(0) = S_0,\ I(0) = I_0,\ R(0) = R_0,\ D(0) = D_0\ (see\ Table\ 1). \tag{2}$$

Table 1: Description of symbols used in the model

Symbol	**Description**
$\frac{d}{dt} \equiv \partial_t$	Derivative with respect to time t
$S(t)$	Susceptible population at time t
$I(t)$	Infected population at time t
$R(t)$	Recovered population at time t
$D(t)$	Cumulative death population at time t
N	Total population (assumed constant)
α	Infection rate
β	Rate at which recovered become susceptible
γ	Natural death rate
ϵ	Ebola-induced death rate
δ	Recovery rate

The classical model effectively represents the basic transmission mechanisms. However, it overlooks the memory and hereditary effects that influence disease evolution. To address this limitation, we extend the system to a fractional-order framework using the Caputo derivative. In this work, we study the following fractional-order Ebola virus model (FEVM) for $t > 0$:

$$\begin{cases} \mathcal{D}_t^\sigma S(t) = -\alpha S(t)I(t) + \beta R(t) - \gamma N, \\ \mathcal{D}_t^\sigma I(t) = \alpha S(t)I(t) - \epsilon I(t) - \delta I(t), \\ \mathcal{D}_t^\sigma R(t) = \delta I(t) - \beta R(t), \\ \mathcal{D}_t^\sigma D(t) = \epsilon I(t) + \gamma N, \end{cases} \tag{3}$$

subject to the initial conditions mentioned in (2). $\mathcal{D}_t^\sigma$ denotes the Caputo derivative of order $\sigma \in (0, 1)$, defined by [20]

$$\mathcal{D}_t^\sigma \phi(t) = \int_0^t \frac{(t-z)^{-\sigma}\, \partial_z \phi(z)}{\Gamma(1-\sigma)} dz.$$

Mathematical modeling has significantly contributed to understanding the transmission dynamics of the Ebola virus, evaluating intervention strategies, and predicting outbreak scenarios. Due to the nonlinear and nonlocal characteristics of fractional-order systems, finding exact solutions is typically challenging [13]. Therefore, numerous numerical and semi-analytical techniques have been developed to approximate solutions effectively [15]. Selected contributions include: Pontryagin's maximum principle is used by Bonyah, Badu, and Asiedu-Addo [7] to derive the necessary conditions for optimality in a compartmental Ebola model. These conditions were implemented numerically via a fourth-order Runge–Kutta method within an iterative forward-backward framework. A dual modeling framework, deterministic and stochastic, was explored by Berge et al. [6]. The deterministic system is handled using a standard Runge–Kutta method, while the stochastic variant employs a continuous-time Markov chain to capture the random nature of disease transmission. To model fractional dynamics, Singh [21] developed an iterative numerical scheme based on the Grünwald–Letnikov fractional derivative. In another study, Ahmad, Rafiq, and Abbas [4] investigated the SVEIR model using the classical fourth-order Runge–Kutta method and a nonstandard finite difference scheme. Srivastava et al. developed three Ebola virus models based on the fractal–fractional derivative with power-law, exponential, and Mittag–Leffler kernels. They applied Lagrange polynomial interpolation to construct numerical schemes for each model and compared their behaviors under varying parameters. The conformable fractional differential transform method, a power-series-based technique, was applied by Nazir et al. [19] to obtain approximate solutions of a nonlinear Ebola model. To solve a Caputo-type fractional model, Derakhshan [8] proposed the Sinc–Legendre collocation method, demonstrating high accuracy and numerical stability in fractional-order equations. Lagrange

polynomial interpolation was also used by Adu et al. [3] to approximate the trajectory of a fractional Ebola system, emphasizing the method's capability to capture nonlocal dynamics. In a separate approach, Abbas et al. [2] incorporated the Grünwald–Letnikov derivative into the classical fourth-order Runge–Kutta framework to solve a fractional-order Ebola model. Abah et al. [1] utilized the homotopy perturbation method to analyze a nonlinear Ebola model incorporating mitigation strategies such as quarantine and public awareness.

Motivated by the existing literature, we have conducted a qualitative study on an Ebola virus model involving an arbitrary-order derivative, focusing on its analytical solution existence, uniqueness, and stability. Additionally, we propose an efficient iterative difference scheme based on the standard L1 technique to approximate the solution of the nonlinear system (3). Theoretical analysis and illustrative test examples validate the accuracy and efficiency of the proposed method. The structure of the paper is as follows: The existence of the analytical solution of (3) is discussed in Section 2, while Section 3 establishes its uniqueness. Stability results for (3) are derived in Section 3.1. The construction of the numerical scheme for solving (3) is provided in Section 4. Section 5 focuses on numerical simulations, and concluding remarks are presented in Section 6.

2 Existence of the solution

In this section, we analyze the existence of a solution for the FEVM using fixed-point techniques. Applying the Riemann–Liouville fractional integral operator to both sides of system (3), we obtain the equivalent integral formulation:

$$\begin{cases} S(t) = S_0 + \displaystyle\int_0^t \frac{G_1(z, S(z))}{\Gamma(\sigma)(t-z)^{\sigma-1}}\, dz, \quad I(t) = I_0 + \int_0^t \frac{G_2(z, I(z))}{\Gamma(\sigma)(t-z)^{\sigma-1}}\, dz, \\ R(t) = R_0 + \displaystyle\int_0^t \frac{G_3(z, R(z))}{\Gamma(\sigma)(t-z)^{\sigma-1}}\, dz, \quad D(t) = D_0 + \int_0^t \frac{G_4(z, D(z))}{\Gamma(\sigma)(t-z)^{\sigma-1}}\, dz, \end{cases}$$

where S_0, I_0, R_0, D_0 are the given initial conditions, and the nonlinear functions $G_i(t, \cdot)$ are defined as

$$\begin{cases} G_1(t, S(t)) = -\alpha S(t) I(t) + \beta R(t) - \gamma N, \\ G_2(t, I(t)) = \alpha S(t) I(t) - \epsilon I(t) - \delta I(t), \\ G_3(t, R(t)) = \delta I(t) - \beta R(t), \quad G_4(t, D(t)) = \epsilon I(t) + \gamma N. \end{cases}$$

Assumption (C_1) : We assume that the functions $S(z), I(z), R(z), D(z), S^1(z), I^1(z), R^1(z), D^1(z) \in L^1[0,1]$, and that the following bounds hold for some positive real constants q_1, q_2, q_3:

$$\|I\| \leq q_1, \quad \|S\| \leq q_2, \quad \|R\| \leq q_3.$$

Theorem 1. The kernels G_1, G_2, G_3, G_4 defined in the FEVM satisfy the Lipschitz conditions under the assumption (C_1), provided that $0 \leq \eta_i < 1$ where $i = 1, 2, 3, 4$.

Proof. First, we prove that the kernel $G_1(t, S)$ satisfies the Lipschitz condition. We compute

$$\begin{aligned}\|G_1(t, S^1) - G_1(t, S^2)\| &= \| - \alpha S^1 I + \beta R - \gamma N - (-\alpha S^2 I + \beta R - \gamma N)\| \\ &= \|\alpha I(S^2 - S^1)\| \leq \alpha q_1 \|S^2 - S^1\| \leq \eta_1 \|S^2 - S^1\|,\end{aligned}$$

where $\eta_1 = \alpha q_1$. Thus, G_1 satisfies the Lipschitz condition provided $\eta_1 < 1$. Next, we consider the kernel $G_2(t, I)$

$$\begin{aligned}\|G_2(t, I^1) - G_2(t, I^2)\| &= \|\alpha S I^1 - \epsilon I^1 - \delta I^1 - (\alpha S I^2 - \epsilon I^2 - \delta I^2)\| \\ &= \|(\alpha S - \delta - \epsilon)(I^1 - I^2)\| \leq (\alpha q_2 + \delta + \epsilon)\|I^1 - I^2\| \\ &\leq \eta_2 \|I^1 - I^2\|,\end{aligned}$$

where $\eta_2 = \alpha q_2 + \epsilon + \delta$. Now, for the kernel $G_3(t, R)$

$$\begin{aligned}\|G_3(t, R^1) - G_3(t, R^2)\| &= \|\delta I - \beta R^1 - (\delta I - \beta R^2)\| \leq \beta \|R^1 - R^2\| \\ &\leq \eta_3 \|R^1 - R^2\|,\end{aligned}$$

where $\eta_3 = \beta$. Finally, for $G_4(t, D)$, we have

$$\|G_4(t, D^1) - G_4(t, D^2)\| = \|\epsilon I + \gamma N - (\epsilon I + \gamma N)\| = 0.$$

Thus G_4 is constant with respect to D, and hence Lipschitz condition with $\eta_4 = 0$. Therefore, all kernels G_i satisfy the Lipschitz condition with constants $\eta_i < 1$ for $i = 1, 2, 3, 4$, which completes the proof. □

Now, we reformulate the system using the kernels G_i, assuming zero initial conditions $S(0) = I(0) = R(0) = D(0) = 0$. Then, the system becomes

$$\begin{cases} S(t) = \int_0^t \frac{G_1(z, S(z))}{\Gamma(\sigma)(t-z)^{1-\sigma}}\, dz, & I(t) = \int_0^t \frac{G_2(z, I(z))}{\Gamma(\sigma)(t-z)^{1-\sigma}}\, dz, \\ R(t) = \int_0^t \frac{G_3(z, R(z))}{\Gamma(\sigma)(t-z)^{1-\sigma}}\, dz, & D(t) = \int_0^t \frac{G_4(z, D(z))}{\Gamma(\sigma)(t-z)^{1-\sigma}}\, dz. \end{cases}$$

Let us define the following recursive sequences to approximate the solution:

$$\begin{cases} S_k(t) = \int_0^t \frac{G_1(z, S_{k-1}(z))}{\Gamma(\sigma)(t-z)^{1-\sigma}}\, dz, & I_k(t) = \int_0^t \frac{G_2(z, I_{k-1}(z))}{\Gamma(\sigma)(t-z)^{1-\sigma}}\, dz, \\ R_k(t) = \int_0^t \frac{G_3(z, R_{k-1}(z))}{\Gamma(\sigma)(t-z)^{1-\sigma}}\, dz, & D_k(t) = \int_0^t \frac{G_4(z, D_{k-1}(z))}{\Gamma(\sigma)(t-z)^{1-\sigma}}\, dz, \end{cases} \tag{4}$$

where $S_0(t), I_0(t), R_0(t), D_0(t) \equiv 0$, initialized by the given initial conditions.

Theorem 2. The FEVM (3) admits a solution if the following condition holds:

$$\eta = \max\{\eta_1, \eta_2, \eta_3, \eta_4\} < 1.$$

Proof. We begin by estimating the difference between two successive approximations of the susceptible population as follows:

$$\begin{aligned} \|DS_{k+1}(t)\| &= \|S_{k+1}(t) - S_k(t)\| \\ &= \left\| \int_0^t \frac{[G_1(z, S_k(z)) - G_1(z, S_{k-1}(z))]\, dz}{\Gamma(\sigma)(t-z)^{1-\sigma}} \right\| \\ &\leq \int_0^t \frac{\|G_1(z, S_k(z)) - G_1(z, S_{k-1}(z))\|\, dz}{\Gamma(\sigma)(t-z)^{1-\sigma}}. \end{aligned}$$

Similarly, for the infected population,

$$\begin{aligned} \|DI_{k+1}(t)\| &= \|I_{k+1}(t) - I_k(t)\| \\ &= \left\| \int_0^t \frac{[G_2(z, I_k(z)) - G_2(z, I_{k-1}(z))]\, dz}{\Gamma(\sigma)(t-z)^{1-\sigma}} \right\| \end{aligned}$$

$$\leq \int_0^t \frac{\|G_2(z, I_k(z)) - G_2(z, I_{k-1}(z))\|\, dz}{\Gamma(\sigma)(t-z)^{1-\sigma}}.$$

For the recovered population,

$$\begin{aligned}\|DR_{k+1}(t)\| &= \|R_{k+1}(t) - R_k(t)\| \\ &= \left\| \int_0^t \frac{[G_3(z, R_k(z)) - G_3(z, R_{k-1}(z))]\, dz}{\Gamma(\sigma)(t-z)^{1-\sigma}} \right\| \\ &\leq \int_0^t \frac{\|G_3(z, R_k(z)) - G_3(z, R_{k-1}(z))\|\, dz}{\Gamma(\sigma)(t-z)^{1-\sigma}}.\end{aligned}$$

For the death compartment,

$$\|DD_{k+1}(t)\| = \|D_{k+1}(t) - D_k(t)\| = \left\| \int_0^t \frac{[G_4(z, D_k(z)) - G_4(z, D_{k-1}(z))]}{\Gamma(\sigma)(t-z)^{1-\sigma}} dz \right\| = 0.$$

Now, we show the convergence of the sequences using the recursive bound. For instance,

$$\|S_{n+1}(t) - S(t)\| = \left\| \int_0^t \frac{[G_1(z, S_n(z)) - G_1(z, S(z))]}{\Gamma(\sigma)(t-z)^{1-\sigma}} dz \right\| \leq \frac{\eta_1 t^\sigma}{\Gamma(1+\sigma)} \|S_n - S\|.$$

Iterating the above inequality leads to

$$\|S_{n+1}(t) - S(t)\| \leq \left(\frac{\eta_1 t^\sigma}{\Gamma(1+\sigma)} \right)^n \|S_1 - S\|.$$

Similarly, we get

$$\begin{aligned}\|I_{n+1}(t) - I(t)\| &\leq \left(\frac{\eta_2 t^\sigma}{\Gamma(1+\sigma)} \right)^n \|I_1 - I\|, \\ \|R_{n+1}(t) - R(t)\| &\leq \left(\frac{\eta_3 t^\sigma}{\Gamma(1+\sigma)} \right)^n \|R_1 - R\|, \\ \|D_{n+1}(t) - D(t)\| &= 0.\end{aligned}$$

Since $\eta = \max\{\eta_1, \eta_2, \eta_3, \eta_4\} < 1$, it follows that all sequences converge uniformly. Hence the system admits a unique continuous solution. □

3 Uniqueness of the solution

Next, we demonstrate the uniqueness of solutions for the FEVM.

Theorem 3 (Uniqueness of solution)**.** The FEVM (3) possesses a unique solution if the following inequality is satisfied:

$$\frac{\eta_i}{\Gamma(\sigma)} < 1 \quad \text{for} \quad i = 1, 2, 3, 4.$$

Proof. Assume, to the contrary, that there exists a distinct solution to the system (3), denoted by $S^\star(t), I^\star(t), R^\star(t), D^\star(t)$. Then, both this solution and the original one must satisfy the corresponding integral formulations of the model

$$S(t) = \int_0^t \frac{G_1(z, S(z))dz}{\Gamma(\sigma)(t-z)^{1-\sigma}}, \qquad S^\star(t) = \int_0^t \frac{G_1(z, S^\star(z))dz}{\Gamma(\sigma)(t-z)^{1-\sigma}}.$$

Subtracting and taking norms, we get

$$\begin{aligned} \|S(t) - S^\star(t)\| &= \left\| \int_0^t \frac{[G_1(z, S(z)) - G_1(z, S^\star(z))]\, dz}{\Gamma(\sigma)(t-z)^{1-\sigma}} \right\| \\ &\leq \int_0^t \frac{\|G_1(z, S(z)) - G_1(z, S^\star(z))\|\, dz}{\Gamma(\sigma)(t-z)^{1-\sigma}} \leq \frac{\eta_1 t^\sigma}{\Gamma(1+\sigma)} \|S - S^\star\|. \end{aligned}$$

If $\frac{\eta_1 t^\sigma}{\Gamma(1+\sigma)} < 1$, then it follows that $\|S - S^\star\| = 0$. Hence $S(t) = S^\star(t)$ for $t \in [0, T]$. Similarly, for the infected compartment,

$$\begin{aligned} \|I(t) - I^\star(t)\| &\leq \int_0^t \frac{\|G_2(z, I(z)) - G_2(z, I^\star(z))\| dz}{\Gamma(\sigma)(t-z)^{1-\sigma}} \leq \frac{\eta_2 t^\sigma}{\Gamma(1+\sigma)} \|I - I^\star\| \\ &\Rightarrow I(t) = I^\star(t). \end{aligned}$$

For the recovered compartment,

$$\begin{aligned} \|R(t) - R^\star(t)\| &\leq \int_0^t \frac{\|G_3(z, R(z)) - G_3(z, R^\star(z))\| dz}{\Gamma(\sigma)(t-z)^{1-\sigma}} \leq \frac{\eta_3 t^\sigma}{\Gamma(1+\sigma)} \|R - R^\star\| \\ &\Rightarrow R(t) = R^\star(t). \end{aligned}$$

Finally, since G_4 is constant with respect to D, we have $\|D(t) - D^\star(t)\| = 0 \Rightarrow D(t) = D^\star(t)$.

This however means, all components of the solution coincide. This proves that the solution is unique. □

3.1 Stability of the solution

Definition 1 (Hyers–Ulam stability [14])**.** The fractional integral system described in (4) is said to be stable if there exist constants $\delta_i > 0$ for $i = 1, 2, 3, 4$, such that for every $\zeta_i > 0$, the following inequalities hold:

$$\left| S(z) - \int_0^t \frac{G_1(z, S(z))dz}{\Gamma(\sigma)(t-z)^{1-\sigma}} \right| \leq \zeta_1, \left| I(z) - \int_0^t \frac{G_2(z, I(z))dz}{\Gamma(\sigma)(t-z)^{1-\sigma}} \right| \leq \zeta_2,$$
$$\left| R(z) - \int_0^t \frac{G_3(z, R(z))dz}{\Gamma(\sigma)(t-z)^{1-\sigma}} \right| \leq \zeta_3, \left| D(z) - \int_0^t \frac{G_4(z, D(z))dz}{\Gamma(\sigma)(t-z)^{1-\sigma}} \right| \leq \zeta_4.$$

Then, there exist functions $\bar{S}(z), \bar{I}(z), \bar{R}(z), \bar{D}(z)$ satisfying the inequalities

$$\left| \bar{S}(z) - \int_0^t \frac{G_1(z, \bar{S}(z))dz}{\Gamma(\sigma)(t-z)^{1-\sigma}} \right| \leq \zeta_1, \left| \bar{I}(z) - \int_0^t \frac{G_2(z, \bar{I}(z))dz}{\Gamma(\sigma)(t-z)^{1-\sigma}} \right| \leq \zeta_2,$$
$$\left| \bar{R}(z) - \int_0^t \frac{G_3(z, \bar{R}(z))dz}{\Gamma(\sigma)(t-z)^{1-\sigma}} \right| \leq \zeta_3, \left| \bar{D}(z) - \int_0^t \frac{G_4(z, \bar{D}(z))dz}{\Gamma(\sigma)(t-z)^{1-\sigma}} \right| \leq \zeta_4,$$

such that

$$\left| S(z) - \bar{S}(z) \right| = \int_0^t \frac{\left| G_1(z, S(z)) - G_1(z, \bar{S}(z)) \right| dz}{\Gamma(\sigma)(t-z)^{1-\sigma}} \leq \frac{\eta_1 t^\sigma}{\Gamma(1+\sigma)} \left\| S - \bar{S} \right\|.$$

Let $\zeta_1^\star = \frac{t^\sigma}{\Gamma(1+\sigma)} \left\| S - \bar{S} \right\|$ and $\delta_1 = \eta_1$, then we have $\left| S(z) - \bar{S}(z) \right| \leq \zeta_1^\star \delta_1$.

Similarly, we obtain

$$\left| I(z) - \bar{I}(z) \right| \leq \zeta_2^\star \delta_2, \quad \left| R(z) - \bar{R}(z) \right| \leq \zeta_3^\star \delta_3, \quad \left| D(z) - \bar{D}(z) \right| \leq \zeta_4^\star \delta_4.$$

Theorem 4 (Hyers-Ulam stability)**.** Under the given assumptions, the FEVM (3) is stable.

Proof. According to the uniqueness Theorem 3, the model (3) has a unique solution $S(z), I(z), R(z), D(z)$. Let the approximate solution of the model be denoted by $S^\star(z), I^\star(z), R^\star(z)$ and $D^\star(z)$. Then,

we have

$$|S(z) - S^\star(z)| = \int_0^t \frac{|G_1(z, S(z)) - G_1(z, S^\star(z))|\, dz}{\Gamma(\sigma)(t-z)^{1-\sigma}} \leq \frac{\eta_1 t^\sigma}{\Gamma(1+\sigma)} \|S - S^\star\|.$$

Let $\eta_1^\star = \frac{t^\sigma}{\Gamma(1+\sigma)} \|S - S^\star\|$ and $\delta_1^\star = \eta_1$. Then $|S(z) - S^\star(z)| \leq \eta_1^\star \delta_1^\star$. Similarly, for $I(z)$

$$|I(z) - I^\star(z)| = \int_0^t \frac{|G_2(z, I(z)) - G_2(z, I^\star(z))|\, dz}{\Gamma(\sigma)(t-z)^{1-\sigma}} \leq \frac{\eta_2 t^\sigma}{\Gamma(1+\sigma)} \|I - I^\star\|.$$

Let $\eta_2^\star = \frac{t^\sigma}{\Gamma(1+\sigma)} \|I - I^\star\|$, and $\delta_2^\star = \eta_2$. Then $|I(z) - I^\star(z)| \leq \eta_2^\star \delta_2^\star$. For $R(z)$

$$|R(z) - R^\star(z)| = \int_0^t \frac{|G_3(z, R(z)) - G_3(z, R^\star(z))|}{\Gamma(\sigma)(t-z)^{1-\sigma}} dz \leq \frac{\eta_3 t^\sigma}{\Gamma(1+\sigma)} \|R - R^\star\|.$$

Let $\eta_3^\star = \frac{t^\sigma}{\Gamma(1+\sigma)} \|R - R^\star\|$, and $\delta_3^\star = \eta_3$. Then $|R(z) - R^\star(z)| \leq \eta_3^\star \delta_3^\star$. Finally, for $D(z)$, since G_4 is independent of D, we trivially have $|D(z) - D^\star(z)| = 0$, which satisfies Hyers–Ulam stability with $\eta_4^\star = 0$, $\delta_4^\star = 0$. Thus, all state variables satisfy the Hyers–Ulam condition, and the model is Hyers–Ulam stable. □

4 The discretized problem

Let M be a positive integer and define a uniform partition of the interval $[0, T]$, $T > 0$ as $\{t_j = j\tau \mid j = 0, 1, \ldots, M\}$, where the step size is $\tau = T/M$. The Caputo fractional derivative of order σ applied to $S(t)$ at the grid point t_j for $j = 1, 2, \ldots, M$ is expressed as

$$\mathcal{D}_t^\sigma S(t_j) = \frac{1}{\Gamma(1-\sigma)} \sum_{k=0}^{j-1} \int_{t_k}^{t_{k+1}} (t_j - s)^{-\sigma} \partial_s S(s)\, ds,$$

which can be approximated using the L1 scheme [16] as

$$\begin{aligned} \mathcal{D}_M^\sigma S(t_j) &= \frac{1}{\Gamma(1-\sigma)} \sum_{k=0}^{j-1} \frac{1}{\tau} [S(t_{k+1}) - S(t_k)] \int_{t_k}^{t_{k+1}} (t_j - s)^{-\sigma} ds \\ &= \sum_{k=0}^{j-1} [S(t_{k+1}) - S(t_k)]\, d_{j-k} \end{aligned}$$

$$= S(t_j)d_1 + \sum_{k=1}^{j-1}(d_{j-k+1} - d_{j-k})S(t_k) - S(t_0)d_j, \tag{5}$$

where $d_p = \frac{\tau^{-\sigma}}{\Gamma(2-\sigma)}[p^{1-\sigma} - (p-1)^{1-\sigma}]$ for $p = 1, 2, \ldots, M$. Similarly, the L1 discretization of $\mathcal{D}_t^\sigma I(t)$, $\mathcal{D}_t^\sigma R(t)$ and $\mathcal{D}_t^\sigma D(t)$ at t_j are given by

$$\begin{aligned}
\mathcal{D}_M^\sigma I(t_j) &= \sum_{k=0}^{j-1} [I(t_{k+1}) - I(t_k)]\, d_{j-k}, \\
\mathcal{D}_M^\sigma R(t_j) &= \sum_{k=0}^{j-1} [R(t_{k+1}) - R(t_k)]\, d_{j-k}, \\
\mathcal{D}_M^\sigma D(t_j) &= \sum_{k=0}^{j-1} [D(t_{k+1}) - D(t_k)]\, d_{j-k}.
\end{aligned}$$

Substituting the above into the model (3), we obtain the discrete system

$$\begin{cases}
\mathcal{D}_M^\sigma S(t_j) = -\alpha S(t_j)I(t_j) + \beta R(t_j) - \gamma N, \\
\mathcal{D}_M^\sigma I(t_j) = \alpha S(t_j)I(t_j) - \epsilon I(t_j) - \delta I(t_j), \\
\mathcal{D}_M^\sigma R(t_j) = \delta I(t_j) - \beta R(t_j), \\
\mathcal{D}_M^\sigma D(t_j) = \epsilon I(t_j) + \gamma N.
\end{cases} \tag{6}$$

Rewriting in simplified form, we get

$$\begin{cases}
(d_1 + \alpha I(t_j))S(t_j) - \beta R(t_j) + \gamma N + \sum_{k=1}^{j-1}(d_{j-k+1} - d_{j-k})S(t_k) - S(t_0)d_j = 0, \\
(d_1 + \epsilon + \delta - \alpha S(t_j))I(t_j) + \sum_{k=1}^{j-1}(d_{j-k+1} - d_{j-k})I(t_k) - I(t_0)d_j = 0, \\
(d_1 + \beta)R(t_j) - \delta I(t_j) + \sum_{k=1}^{j-1}(d_{j-k+1} - d_{j-k})R(t_k) - R(t_0)d_j = 0, \\
(d_1)D(t_j) - \epsilon I(t_j) - \gamma N + \sum_{k=1}^{j-1}(d_{j-k+1} - d_{j-k})D(t_k) - D(t_0)d_j = 0.
\end{cases} \tag{7}$$

Define the system compactly for $j = 1, 2, \ldots, M$ as

$$\begin{cases} F_1(S_j, I_j, R_j, D_j) = 0, & F_2(S_j, I_j, R_j, D_j) = 0, \\ F_3(S_j, I_j, R_j, D_j) = 0, & F_4(S_j, I_j, R_j, D_j) = 0, \\ S_j, I_j, R_j, D_j \geq 0, \end{cases} \tag{8}$$

where S_j denotes the approximate value of $S(t)$ at time t_j. Similar notation is used for I_j, R_j, and D_j. The nonlinear algebraic system (8) is solved using the Newton–Raphson method, with the initial guess

$$\begin{bmatrix} S_j^{(0)} \\ I_j^{(0)} \\ R_j^{(0)} \\ D_j^{(0)} \end{bmatrix} = \begin{bmatrix} S_{j-1} \\ I_{j-1} \\ R_{j-1} \\ D_{j-1} \end{bmatrix}.$$

Then, the nth iteration is computed by

$$\begin{bmatrix} S_j^{(n)} \\ I_j^{(n)} \\ R_j^{(n)} \\ D_j^{(n)} \end{bmatrix} = \begin{bmatrix} S_j^{(n-1)} \\ I_j^{(n-1)} \\ R_j^{(n-1)} \\ D_j^{(n-1)} \end{bmatrix} - J_{(n-1)}^{-1} \begin{bmatrix} F_1^{(n-1)} \\ F_2^{(n-1)} \\ F_3^{(n-1)} \\ F_4^{(n-1)} \end{bmatrix},$$

where $J_{(n-1)}$ is the Jacobian matrix computed using partial derivatives of F_i with respect to the unknowns. Finally, the solution at step j is approximated as

$$\begin{bmatrix} S_j \\ I_j \\ R_j \\ D_j \end{bmatrix} \approx \begin{bmatrix} S_j^{(n)} \\ I_j^{(n)} \\ R_j^{(n)} \\ D_j^{(n)} \end{bmatrix}.$$

5 Numerical illustration and discussions

The following test example is presented to validate the accuracy and efficiency of the proposed numerical scheme. All simulations are carried out using MATLAB R2016a.

Example 1. Consider the model problem (3) with initial conditions as given in [21]: $\alpha = 0.01$, $\beta = 0.02$, $\gamma = 0.01$, $N = 1000$, $\epsilon = 0.6$, $\delta = 0.4$, $S(0) = 970$, $I(0) = 30$, $R(0) = 0$, $D(0) = 0$.

To evaluate the model (3), a comparative numerical experiment was conducted using three different fractional orders: 0.99, 0.95, and 0.9. The simulation results for each case are depicted in

Figures 1. Specifically, Figure 1a corresponds to $\sigma = 0.99$, Figure 1b to $\sigma = 0.95$, and Figure 1c to $\sigma = 0.9$. Across all three cases, the system dynamics are qualitatively similar, confirming the consistency and robustness of the proposed method. These observations align with previous results reported in [21]. Further, comparative analysis is presented in Figures 2, which show the influence of varying fractional orders ($\sigma = 0.90$, 0.95, 0.98, and 0.99) on the dynamics of the individual compartments. Figure 2a illustrates the dynamics of the susceptible population $S(t)$, which exhibits a decreasing trend as σ increases. This implies that higher fractional orders slightly accelerate the depletion of the susceptible population. The infected population $I(t)$ in Figure 2b grows sharply at first but then falls to zero more quickly when σ gets closer to 0.99. This indicates that infection is recovered and controlled more quickly at higher fractional orders. The recovered population $R(t)$, shown in Figure 2c, increases monotonically with time and stabilizes more quickly as σ increases, indicating a faster transition from infection to recovery. Finally, the evolution of the cumulative death population $D(t)$ is illustrated in Figure 2d, where a gradual stabilization follows an initially rapid growth. The figure indicates a pronounced increase at higher fractional orders, highlighting the significant influence of σ on mortality accumulation. Although the system's qualitative behavior remains consistent for $0.90 \leq \sigma \leq 0.99$, small changes in σ produce notable quantitative shifts, highlighting the model sensitivity to the fractional order.

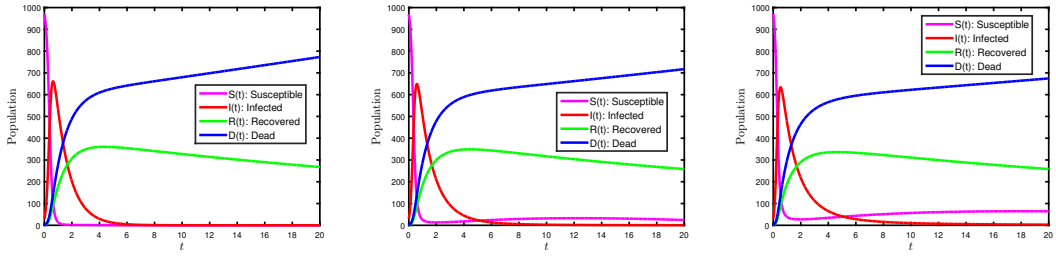

(a) $\sigma = 0.99$ (b) $\sigma = 0.95$ (c) $\sigma = 0.9$

Figure 1: Solutions of $S(t), I(t), R(t)$, and $D(t)$.

6 Conclusion

In this study, we developed and analyzed a FEVM transmission, focusing on the assessment of its long-term dynamics. We examined the existence, uniqueness, and stability of the model solutions using fractional calculus, specifically employing the Caputo derivative. Numerical simulations were carried out using an iterative scheme with initial conditions. To explore the transmission behavior of the Ebola virus, we analyzed the system under varying fractional orders and param-

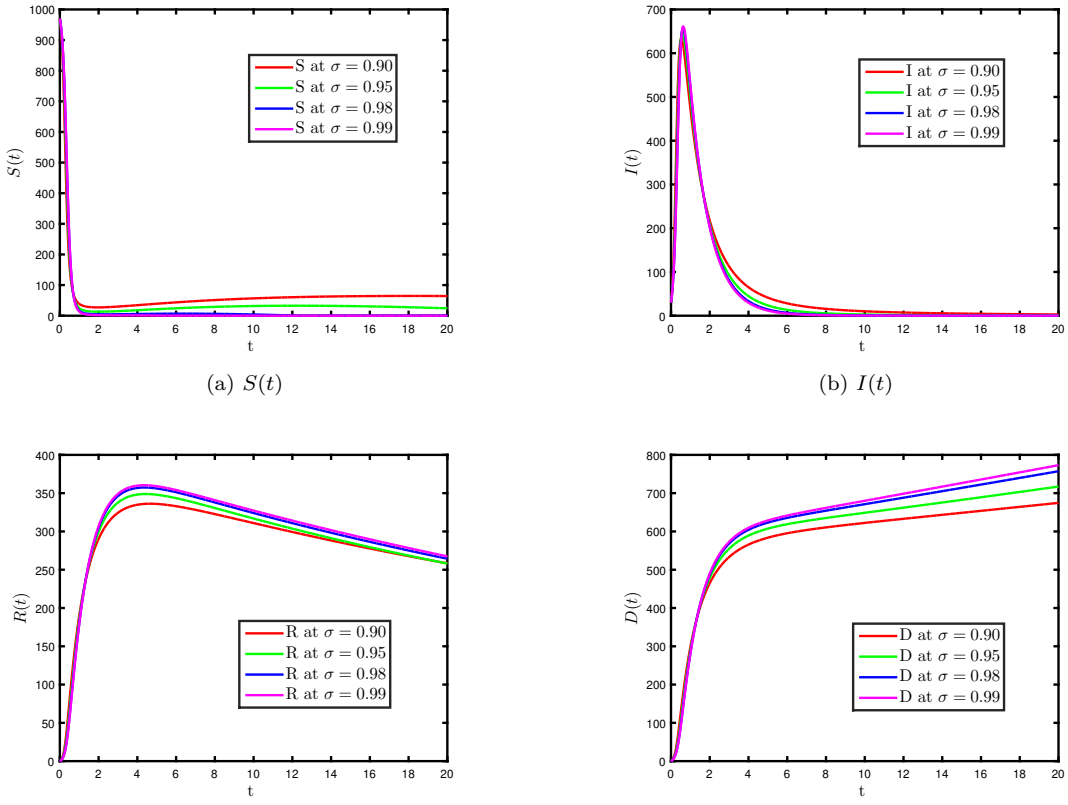

(a) $S(t)$ (b) $I(t)$

(c) $R(t)$ (d) $D(t)$

Figure 2: Comparison of $S(t)$, $I(t)$, $R(t)$, and $D(t)$ for different σ.

eter sensitivities. The results of the numerical experiments illustrate that FEVM yields solutions that are not only consistent with biological expectations but also more flexible and realistic than their integer-order counterparts. These findings underscore the significance of incorporating fractional derivatives into epidemiological modeling, as they offer a more accurate representation of memory and hereditary properties inherent in infectious disease dynamics.

Funding

This research received no external funding.

Conflicts of interest

The authors declare that there are no conflicts of interest.

References

[1] Abah, R.T., Zhiri, A.B., Oshinubi, K. and Adeniji, A. *Mathematical analysis and simulation of Ebola virus disease spread incorporating mitigation measures*. Frankl. Open, 6 (2024), 100066.

[2] Abbas, N., Zanib, S.A., Ramzan, S., Nazir, A. and Shatanawi, W. *A conformable mathematical model of Ebola virus disease and its stability analysis*. Heliyon, 10(16) (2024) e35818.

[3] Adu, I.K., Wireko, F.A., Sebil, C. and Asamoah, J.K.K. *A fractal–fractional model of Ebola with reinfection*. Results Phys., 52 (2023), 106893.

[4] Ahmad, W., Rafiq, M. and Abbas, M. *Mathematical analysis to control the spread of Ebola virus epidemic through voluntary vaccination*. Eur. Phys. J. Plus, 135(10) (2020), 775.

[5] Saini, G., Ghosh, B., Chand, S. and Mohapatra, J. *An iterative-based difference scheme for nonlinear fractional integro-differential equations of Volterra type*. Partial Differ. Equ. Appl. Math., 13 (2025), 101138.

[6] Berge, T., Chapwanya, M., Lubuma, J.S. and Terefe, Y.A. *A mathematical model for Ebola epidemic with self-protection measures*. J. Biol. Syst., 26(1) (2018), 107–131.

[7] Bonyah, E., Badu, K. and Asiedu-Addo, S.K. *Optimal control application to an Ebola model*. Asian Pac. J. Trop. Biomed., 6(4) (2016), 283–289.

[8] Derakhshan, M.H. *The stability analysis and numerical simulation based on Sinc Legendre collocation method for solving a fractional epidemiological model of the Ebola virus*. Partial Differ. Equ. Appl. Math., 3 (2021), 100037.

[9] Ghosh, B. and Mohapatra, J. *Numerical simulation for two species time fractional weakly singular model arising in population dynamics*. Int. J. Model. Simul., 45(4) (2025), 1383–1396.

[10] Gunasekar, T., Manikandan, S., Govindan, V., Ahmad, J., Emam, W. and Al-Shbeil, I. *Symmetry analyses of epidemiological model for Monkeypox virus with Atangana–Baleanu fractional derivative*. Symmetry, 15(8) (2023), 1605.

[11] Gunasekar, T., Manikandan, S., Suba, M. and Akgül, A. *A fractal–fractional mathematical model for COVID-19 and tuberculosis using Atangana–Baleanu derivative*. Math. Comput. Model. Dyn. Syst., 30(1) (2024), 857–881.

[12] Gunasekar, T., Manikandan, S., Haque, S., Suba, M. and Mlaiki, N. *Fractal–fractional mathematical modeling of monkeypox disease and analysis of its Ulam–Hyers stability*. Bound. Value Probl., 2025(1) (2025), 20.

[13] Hussain, S., Arora, G. and Kumar, R. *Analytical and numerical treatments of a coagulation population balance model*. Chaos Solit. Fractals, 192 (2025), 115974.

[14] Jung, S.M. *Hyers–Ulam stability of linear differential equations of first order*. Appl. Math. Lett., 17(10) (2004), 1135–1140.

[15] Kaushik, S., Kumar, R. and da Costa, F.P. *Theoretical analysis of a discrete population balance model with sum kernel*. Port. Math., 80(3) (2023), 343–367.

[16] Lin, Y. and Xu, C. *Finite difference/spectral approximations for the time-fractional diffusion equation*. J. Comput. Phys., 225(2) (2007), 1533–1552.

[17] Mainardi, F. *Fractional calculus and waves in linear viscoelasticity: An introduction to mathematical models*. World Scientific, 2010.

[18] Manikandan, S., Gunasekar, T., Kouidere, A., Venkatesan, K.A., Shah, K. and Abdeljawad, T. *Mathematical modelling of HIV/AIDS treatment using Caputo–Fabrizio fractional differential systems*. Qual. Theory Dyn. Syst., 23(4) (2024), 149.

[19] Nazir, A., Ahmed, N., Khan, U., Mohyud-Din, S.T., Nisar, K.S. and Khan, I. *An advanced version of a conformable mathematical model of Ebola virus disease in Africa*. Alex. Eng. J., 59(5) (2020), 3261–3268.

[20] Podlubny, I. *Fractional Differential Equations*. Academic Press, 1999.

[21] Singh, H. *Analysis for fractional dynamics of Ebola virus model*. Chaos Solit. Fractals, 138 (2020), 109992.

[22] Suba, M., Venkatesan, A., Gunasekar, T., Manikandan, S., Raghavendran, P., Santra, S.S. and Karmakar, S. *Advancing Zika virus control with fractional order optimal control with Wolbachia-infected Aedes aegypti mosquitoes*. In *International Conference on Mathematical Modelling, Applied Analysis and Computation*, Springer, (2024), 160–183.

[23] Yang, X.J., Gao, F. and Ju, Y. *General fractional derivatives with applications in viscoelasticity*. Academic Press, 2020.